Zeitschrift: Helvetica Physica Acta

Band: 56 (1983)

Heft: 1-3

Artikel: Quasi-two-dimensional excitations in GaAs/Al_xGa_1-xAs semiconductor multiple quantum well structures

Autor: Chemla, D.S.

DOI: https://doi.org/10.5169/seals-115405

Helvetica Physica Acta,
Vol. 56 (1983) 607-637

0018-0238/83/010607-31$1.50+0.20/0

Quasi-two-dimensional Excitons in $GaAs/Al_xGa_{1-x}As$ Semiconductor Multiple Quantum Well Structures

D. S. Chemla
Bell Laboratories
Holmdel, New Jersey 07733

ABSTRACT

This article reviews recent studies on excitons in $GaAs/Al_xGa_{1-x}As$ multiple quantum well structures (MQWS). After a theoretical summary, the spectroscopy of quasi-two-dimensional excitons is presented. Experiments at low temperature and high excitation are discussed. Excitons in MQWS can be resolved at room temperature. The behavior of excitons in this unusual temperature range are analyzed and the potential applications to optical signal processing are pointed out.

1. Introduction

The physical properties of two dimensional systems have recently attracted a great deal of attention.[1] In semiconductors quasi-two-dimensional free carrier gases can be obtained in inversion layers at various type of interfaces and in quantum wells. Their electronic and optical properties have been intensively studied.[1]

Quantum wells can be synthesized by growing alternating thin layers of two semiconductors having different band gaps. It was recognized early that Multiple Quantum Well Structures (MQWS) would exhibit novel properties.[2] The discontinuity of the energy gap results in a variation of the conduction and valence bands edges. A schematic of this variation in the case of undoped semiconductors is shown in Figure 1. For proper values of the potential barrier heights, (ΔE_c and ΔE_v), and of the low gap and large gap layer thicknesses, (L_z and L_b), quantization in the direction perpendicular to the layers (z) gives rise to discrete energy levels. If the barrier thickness L_b is large enough to prevent overlap of the exponential tails of the wave functions in adjacent wells, the wells behave independently. To obtain structures with very abrupt interfaces the growth

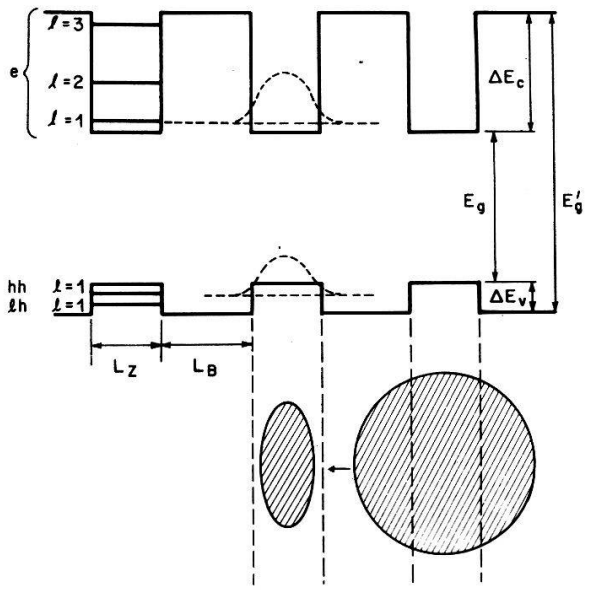

Figure 1: Schematic of the band structure, in real space, of a multiple quantum well structure for undoped materials. The crosshatched circle represents the exciton in the bulk compound. The confinement in thin layers modifies the structure of the exciton which is somehow flattened, and shrinked. This is illustrated by the crosshatched ellips.

process must be controlled down to the atomic scale and the semiconductor components must exhibit very specific compatibilities. The recent progress in growth techniques such as Molecular Beam Epitaxy[3,4] (MBE) has enabled the fabrication of high quality MQWS. The GaAs/$Al_xGa_{1-x}As$ system has been extensively studied and high-quality complex structure involving the two compounds have been successfully prepared.[5]

The optical properties of direct gap semiconductors near the fundamental absorption edge are governed by excitonic effects.[6] Within the framework of the effective mass approximation, the electron-hole system is described in a Hydrogen atom-like fashion with a binding energy $R_y = e^4\mu^*/2\epsilon^2\hbar^2$ and a Bohr radius $a_o = \epsilon\hbar^2/e^2\mu^*$. Here μ^* is the proper electron-hole reduced mass taking into account the valence band structure[7,8] and ϵ is the dielectric constant of the medium.[6] Typical values of these parameters in the case of GaAs are: $R_y = 4.2\ meV$, $2a_o \sim 300$Å.

It is clearly apparent from the above remarks that strong modifications of the excitonic properties can be expected in MQWS when the electrons and holes are effectively confined within layers thin compared to the bulk exciton diameter;[9] $L_z \leqslant 2a_o$. For these conditions exciton propagation cannot occur in the z direction and the exciton structure is modified by the confinement as shown in Figure 1.

This article reviews the unusual aspects of quasi-two-dimensional excitons in $GaAs/Al_xGa_{1-x}As$ Multiple Quantum Well Structures. In Section 2 a brief theoretical background is given. The principal low temperature spectroscopic results are presented in Section 3. The low temperature and the high optical excitation measurements are discussed in Section 4. Finally in Section 5 one of the most unusual aspect of excitons in MQWS, their observation at room temperature, is analyzed. The available experimental results are presented and the potential applications are pointed out.

2. *Theoretical Trends: Absorption in Two and Three Dimensions*

The analysis of the quantization of the states of a particle in a one dimensional rectangular well can be found in most text books on quantum mechanics.[10] An infinitely deep well gives rise to an infinite series of bound states, the energies and wave functions of which are;

$$(1) \qquad E_\ell^\infty = \frac{\hbar^2}{2m^*}\left(\pi\frac{\ell}{L_z}\right)^2 \qquad \zeta_\ell(z) = A_\ell \sin\left(\pi\ell\frac{z}{L_z}\right) .$$

here ℓ is an integer number.

When the well depth is finite the number of bound states is limited. The corresponding wave functions have a sinusoidal dependence in the well and exponential tails in the barrier region. For a symmetric well the energies of the bound states, E_ℓ, are solution of

$$(2) \qquad x^{1/2}\begin{Bmatrix} cotan\ (\pi/2\,x^{1/2}) \\ \tan\ (\pi/2\,x^{1/2}) \end{Bmatrix} = \pm\,(y-x)^{1/2}$$

where $x = (E_\ell/E_1^\infty)$ and $y = (V/E_1^\infty)$ are the normalized energy and potential barrier height. There is always at least one bound state and if the well depth is substantially larger than E_1^∞, the first bound state energies E_ℓ are close to those of the infinitely deep well.

When the particle is confined in the z direction but free in the $[xy]$ plane, two dimensional energy bands are obtained;

(3) $$E_\ell(z) = E_\ell + \frac{\hbar^2}{2m^*}(k_x^2 + k_y^2)$$

The corresponding density of states is a series of step functions, $\theta\ (E-E_\ell)$.

(4) $$g_{2D}(E) = \frac{m^*}{\pi\hbar^2}\sum_\ell \theta\ (E-E_\ell)\ .$$

	3 Dimensions	2 Dimensions
Density of State	$\frac{V}{2\pi^2 a_o^3 R_y}\left(\frac{E-E_g}{R_y}\right)^{1/2}$	$\frac{S}{2\pi a_o^2 R_y}\theta\ (E-E_{11})$
Wave Function	$R_{n,\ell,m}(r)P_\ell^m(\cos\theta)e^{im\phi}$	$R_{n-1/2,m}(r)e^{im\phi}$
Energy	$E_n = -\frac{R_y}{n^2}$	$E_n = -\frac{R_y}{(n-1/2)^2}$
Oscillator strength	$f_n = \frac{2}{\pi m_o a_o^3 \hbar\omega}\frac{\lvert p_{cv}\rvert^2}{n^3}$	$f_n = \frac{2}{\pi m_o a_o^2 \hbar\omega}\frac{\lvert p_{cv}\rvert^2}{(n-1/2)^3}$
Sommerfed Factors	$F(W) = \frac{\pi}{\sqrt{W}}\frac{e^{\pi/\sqrt{W}}}{\sinh(\pi/\sqrt{W})}$	$F(W) = \frac{e^{\pi/\sqrt{W}}}{\cosh(\pi/\sqrt{W})}$
	$F \underset{w\to o}{\to} 2\pi/\sqrt{W}$	$F \underset{w\to o}{\to} 2$
	$F \underset{w\to\infty}{\to} 1$	$F \underset{w\to\infty}{\to} 1$

Table 1: Correspondence between the parameters describing excitons in three dimensional and two dimensional semiconductors. m_o is the free electron mass, W is a reduced and normalized energy $W = (E-E_g)/R_y$ in three dimensions and $W = (E-E_{11})/R_y$ in two dimensions. The Sommerfeld Factors give the enhancement of the absorption in the continuum when the Coulomb interaction is accounted for.

The optical absorption of bulk semiconductors near the fundamental absorption edge is well described within the framework of the effective mass approximation.[6] The absorption of purely-two-dimensional semiconductors can be described in a similar manner. In fact, each step of the analysis can be transposed from the three dimensional to the two dimensional case.[11] It is worth noting that only the motion of the particles is two dimensional, the Coulomb interaction is still three dimensional with a r^{-1} dependence (in a flat universe the Coulomb law would have a logarithmic dependence). The correspondence between the parameters involved in the description of the absorption in the dimensions (3D) and the dimensions (2D) are given in Table I. The principal results are the following. When the Coulomb interaction is neglected the parabolic 3D-absorption edge transforms into a step like 2D-absorption edge with the parabola touching the step at its corner Figure 2. When the Coulomb interaction is considered the hydrogenic spectrum appears. The ground state binding energy of the 2D exciton $B_{1S}^{2D} = -4R_y$ is four times larger than that of the 3D one. The Coulomb enhancement of the absorption above the band gap which gives in 3D an almost flat spectrum, gives in the 2D case a *rise* from the step value far from the gap to a value twice as

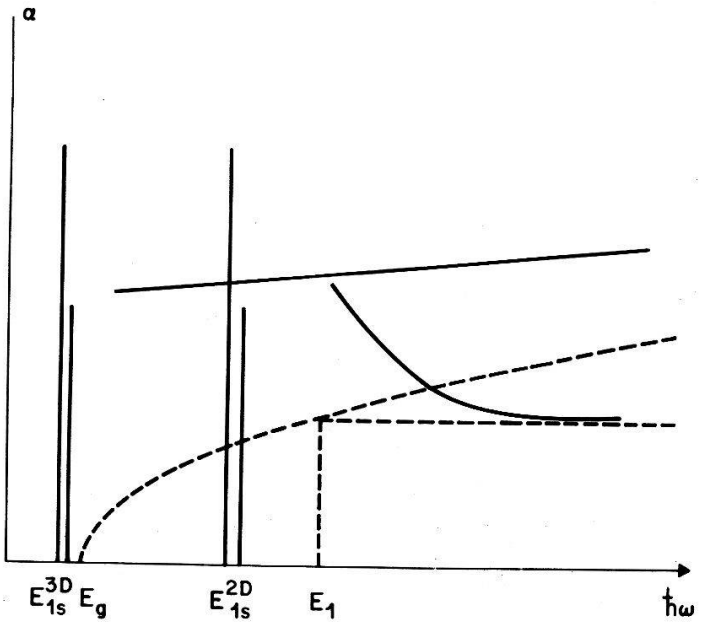

Figure 2: Schematic comparison of the absorption spectra of three dimensional and two dimensional semiconductors close to the fundamental absorption edge. Dash lines: absorption spectra when the Coulomb interaction is neglected. Solid lines: absorption spectra with Coulomb interaction.

large at the ionization limit. Finally the oscillator strengths of the hydrogenic peaks decrease more rapidly in 2D than in 3D i.e., $(n - 1/2)^{-3}$ vs n^{-3}. These results are illustrated in Figure 2.

In thin semiconductor layers because of the *finite thickness and barrier depth* excitons are expected to exhibit properties somehow intermediate between the pure 2D case and the 3D case. The upper valence band of GaAs is the four-fold degenerate multiplet $J = 3/2$. The confinement lifts the degeneracy between the heavy hole (hh) and the light hole (lh) bands. For the usual growth direction, [100] substrate, its symmetry is equivalent to that of a uniaxial stress perpendicular to the layers.[12] This gives rise to different effective masses along the z direction and in the $[xy]$ plane. Near the $k = 0$ point the hole effective mass Hamiltonian can be approximated by;

$$H_{hh}(3/2) = -\frac{\hbar^2}{2m_o}(\gamma_1+\gamma_2)(k_x^2+k_y^2) - \frac{\hbar^2}{2m_o}(\gamma_1-2\gamma_2)k_z^2 \tag{5a}$$

$$H_{lh}(1/2) = -\frac{\hbar^2}{2m}(\gamma_1-\gamma_2)(k_x^2+k_y^2) - \frac{\hbar^2}{2m_o}(\gamma_1+2\gamma_2)k_z^2 \tag{5b}$$

where m_o is the free-electron mass and γ_1, γ_2 are the Luttinger parameters.[13] The effective masses involved in the confinement energy of the holes, Eq. (2), are; $m^*_{hh} = m_o/(\gamma_1-2\gamma_2)$ and $m^*_{lh} = m_o/(\gamma_1+2\gamma_2)$ ($\sim 0.45\, m_o$ and $0.08 m_o$ for GaAs respectively). In the $[xy]$ plane close to $k = 0$ the $M_z = \pm 3/2$ hole is lighter than the $M_z = \pm 1/2$ one; $m_o/(\gamma_1+\gamma_2) < m_o/(\gamma_1-\gamma_2)$. However, it is important to note that Eqs. (5) give a band crossing for $k_{x,y} \sim \pi/L_z$. (In the infinite well depth approximation the crossing occurs exactly at $k_{x,y} = \pi\sqrt{2}/L_z$). In a correct description of the band structure this degeneracy should be lifted. The two bands repel each other giving rise to a non parabolicity. It is only when this effect is taken into account that the band structure is found to vary continuously as a function of L_z between the 2D and 3D limites. In the following we conform our notation to common usage and label the holes; heavy hole (hh) and light hole (lh) by reference to their effective mass in the direction perpendicular to the layers.

The wave functions of the electrons and the holes have the following form;

(6) $$\Psi_{s,l,k}(\bar{r},z) = u_{s,l,k_\perp}(\bar{r})\zeta_{s,l,k_z}(z)\ \exp\ (i\bar{k}.\bar{r})$$

where s is the band index, l the subband index, $u_{s,l,k_\perp}(\bar{r})$ the unit cell Bloch functions and $\zeta_{s,l,k_z}(z)$ is the envelope function introduced by the potential modulation. These functions obey the normalization relations; $\frac{1}{L_z}\int_o^{L_z}\zeta^*_{lk_z}(z)\zeta_{l'k_z}(z)dz = \delta_{ll'}$ and $\frac{1}{\Omega}\int u^*_{s,k_\perp}(\bar{r})u_{s',k_\perp}(\bar{r})d\bar{r} = \delta_{ss'}$. If the envelope function in the conduction band and in the valence band are the same, the transition moment involved in an absorption matrix element is

$$<\Psi_{s,l,k}\ |\bar{A}\cdot\bar{p}|\Psi_{s',l',k'}> \propto(\frac{1}{\Omega}\int u^*_{sk_\perp}\nabla u_{s'k_\perp}dr + \int u^*_{sk_\perp} i\bar{k}.\bar{r}\, u_{s'k_\perp}\, dr)\ \delta_{ll'}$$

(7) $$+ (\frac{1}{L_z}\int \zeta^*_{lk_z}\nabla\zeta_{l'k_z}\, dz)\ \delta_{ss'}\ ,$$

which implies the important selection rule for valence band-conduction band transitions

(8) $$\Delta l = 0\ .$$

In a bulk semiconductor the exciton is built up from the electron and the isotropic part of the hole; the d-symmetry part of the hole Hamiltonian is treated as a perturbation.[7,8] The reduced mass of the exciton in 3D is

(9a) $$\frac{1}{\mu^*} = \frac{1}{m_e^*} + \frac{\gamma_1}{m_o}\ .$$

From Eq. (5) we see that in a quasi-2D layers there are two excitons, involving an electron and respectively the heavy and light holes. Assuming that the $k \sim 0$ masses of Eqs. (5) can be used for the exciton the reduced masses are found to be;

(9b) $$\frac{1}{\mu^*_\pm} = \frac{1}{m^*_e} + \frac{\gamma_1 \pm \gamma_2}{m_o} = \frac{1}{m^*_e} + (1 \mp \frac{1}{2}) \frac{1}{2m^*_{hh}} + (1 \pm \frac{1}{2}) \frac{1}{2m^*_{lh}}$$

In $GaAs/Al_xGa_{1-x}As$ MQWS[14]; $\mu^*_+ \sim 0.04\, m_o$, $\mu^*_- \sim 0.05\, m_o$, and $R_{y_+} \sim 3.7\, meV$ $R_{y_-} \sim 4.5\, meV$. The $e-hh$ and $e-lh$ excitons are expected to be predominately of $M_z = \pm 3/2$ and $M_z = \pm 1/2$ character, respectively.

The natural parameter for measuring the amount of 2D-nature of an exciton is L_z/a_o. For very thick layers ($L_z/a_o > 1$) nearly 3D-exciton effects are expected. Conversely for very thin layers ($L_z/a_o << 1$) excitons approach their 2D limit. In this case, the difference between the true Coulomb Hamiltonian and the 2D one;

$$H' = \frac{e^2}{\epsilon} \left[(x^2+y^2)^{-1/2} - (x^2+y^2+z^2)^{-1/2} \right]$$

can be treated as a perturbation.[15] Its magnitude $<H'> \sim R_y (L_z/a_o)^2$ indicates that the binding energy B_{1S} is very sensitive to the finite well thickness near the 2D limit. In the intermediate range ($L_z/a_o \sim 1$) the confinement squeezes the electron and the hole in one direction and thereby increases the binding energy over that of a bulk excition. The dependence of B_{1S} can be calculated using variational procedures.[14,16] It is found that the confinement enhancement is small for $L_z/a_o > 2.5$, but it is substantial in the range $1/2 < L_z/a_o < 2$, in fact for $L_z/a_o \sim 1$; $B_{1S} \sim -2R_y$.

To summarize this section we can say that in direct gap semiconductors MQWS, the absorption spectrum is expected to present a structure consisting of a series of steps corresponding to valence subbands-conduction subband transitions obeying the selection role $\Delta l = 0$. Each of these transitions gives two steps one for the *lh* and one for the *hh* subbands, both presenting an excitonic feature. The results of this brief introduction should be considered with caution when considering the details of the effects the confinement on the band structure.

3. Spectroscopy of Excitons in Multiple Quantum Well Structures:

R. Dingle and coworkers performed the first spectroscopic studies of the absorption in MQWS close to the fundamental edge.[12,17] Using MBE they were among the first to grow GaAs/$Al_xGa_{1-x}As$ MQWS with the extremely high purity ($\sim 10^{15} cm^{-3}$) necessary to observe extrinsic excitonic effects. They studied a set of samples with L_z in the range 100Å – 500Å, $x \sim 0.2 - 0.3$ and barrier thicknesses ($L_b \sim$ 250Å) much larger than the penetration length of the wave functions in the large gap compound ($\sim$ 20 – 25Å). They observed the expected step like structure with double exciton peaks for the few first transitions, as shown in Figure 3. Using the effective masses of Eq. (5), defined by the Luttinger parameters of the bulk GaAs, and the layer thicknesses as determined from the growth conditions, they deduced from the comparison of their

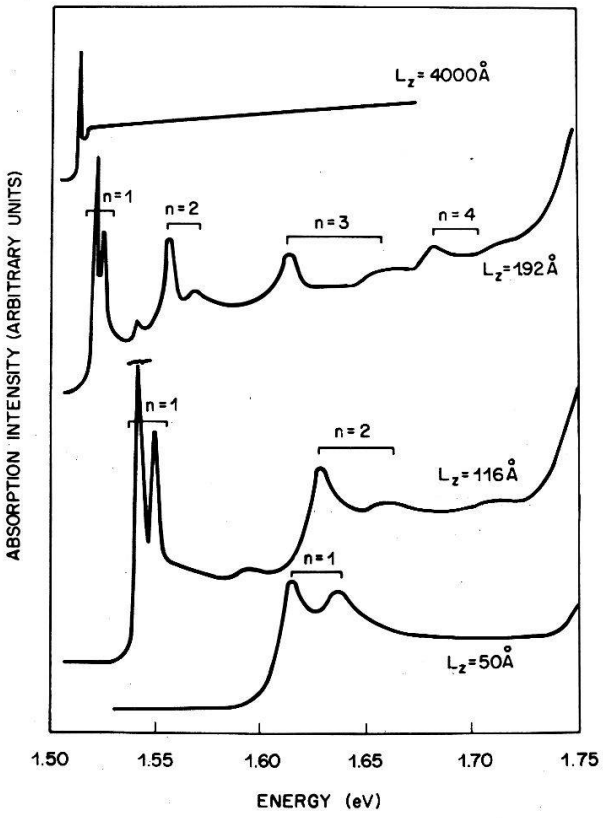

Figure 3: Optical absorption for a 4000Å GaAs film and multiple quantum well structures with GaAs layer thicknesses; L_z = 192Å, 116Å, 50Å, and $Al_{.25}Ga_{.75}As$ layer thicknesses $L_b \sim$ 200Å. (After Ref. [5]).

spectra and the theory, Eq. (2), the only unknown parameters: the depths of the potential barriers at the conduction and valence band edges. This important result fixes how the band gap discontinuity is shared by the two bands.[9]

$$(10) \qquad \frac{\Delta E_c}{\Delta E_g} = 0.85 \pm 0.03 \qquad \frac{\Delta E_v}{\Delta E_g} = 0.15 \pm 0.03 \ .$$

The major part of the discontinuity occurs in the conduction band. The holes are much less confined than the electrons, so that for the light holes only a few states are bounded. This explains why the double exciton structure is only observed in the first transitions.

Intersubband transitions, $\Delta l \neq 0$, are forbidden in one photon processes but can be observed by electronic resonant Raman scattering.[18-20]

R. C. Miller, C. Weisbuch, and coworkers have extensively studied excitons in $GaAs/Al_xGa_{1-x}As$ MQWS by use of luminescence techniques.[14,21-25] The first striking aspect of luminescence in MQWS is the weakness of the extrinsic spectrum which is one to two orders of magnitude weaker than the intrinsic exciton luminescence. This contrasts strongly with bulk GaAs, where bound exciton luminescence and impurity assisted processes dominate. Using spin polarization techniques R. C. Miller, C. Weisbuch, et al[21,22] were able to assign the low energy and high energy exciton peaks to *hh* and *lh* valence bands to conduction band transitions respectively. These experiments confirm the $M_z = \pm 3/2$ and $M_z = \pm 1/2$ character of the *hh* and *lh* bands. The width of the excitonic luminescence peak is found to increase when L_z decreases.[22] This result is interpreted as due to an inhomogeneous broadening of the transition induced by fluctuations of the layer thickness. C. Weisbuch et al[22,23] deduced from their measurements that the $GaAs/Al_xGa_{1-x}As$ interfaces obtained by MBE growth have an island like structure, the islands being approximately one monolayer high and $\lesssim$ 300Å wide. The influence of the layer thickness variation on the exciton width is confirmed by the observation of R. C. Miller et al,[21] who found that it varies approximately as l^2.

The precise value of the ground state binding energy is usually difficult to determine because of the inaccuracy on the position of the continuum edge. In a careful study of photoluminescence R. C. Miller et al[14] observed transitions from the ground state (1S) and the first excited state (2S) of both the $e-hh$ and $e-lh$ excitons. From the measured value of $B_{2S} - B_{1S}$, they deduced the ground state binding energy. This is the first experimental determination of the confinement effect on B_{1S} in layers with finite thickness. Their experimental results are shown in Figure 4, together with a theoretical fit they obtained using a variational procedure. The binding energy is found to vary smoothly between $-4R_y$ and $-R_y$ as discussed in Section 1; the $e-lh$ exciton is more tightly bound than the $e-hh$ one confirming the values of the effective masses in the plane of the layers. At high excitation forbidden transition ($\Delta l = odd$) can be observed,[21,25] they arise most likely through three body interactions.

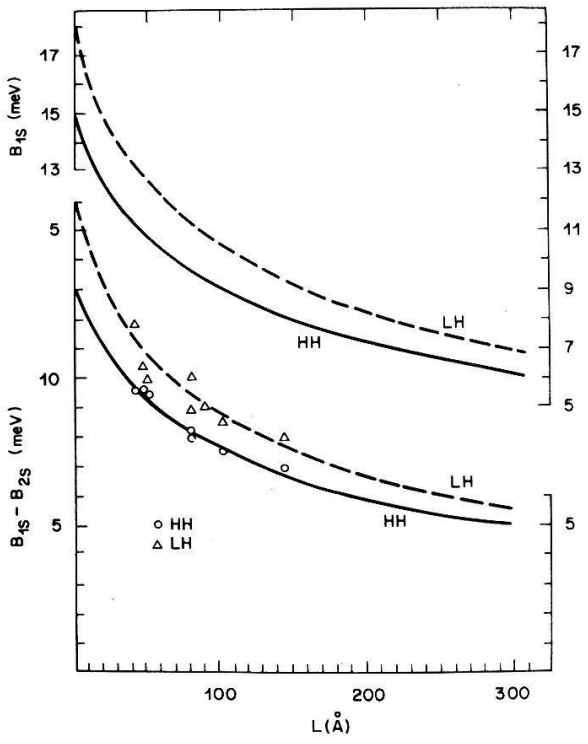

Figure 4: Separation between the 1S and 2S photo luminescence peak ($B_{1S}-B_{2S}$) for the $e-hh$ and $e-lh$ quasi-two-dimensional exciton as a function of the GaAs layer thickness. Binding energy of the ground state B_{1S} as a function of the GaAs layer thickness. (After Ref. [14]).

In bulk GaAs observation of biexcitons have not been reported most likely because of their very small binding energy which is estimated to be of the order of 0.1 meV.[26] As in the case of excitons the binding energy of biexcitons is expected to be increased by confinement in thin layers. Recently R. C. Miller et al[27] have observed the appearance of a new peak near the exciton edge of the photoluminescence of several MQWs, whose dependences upon excitation intensity, polarization and temperature suggest that it originates form biexciton recombination. The binding energy they deduced from their experiment ($\sim$ 1 *meV*) is more than one order of magnitude larger than the estimates for 3D GaAs and is in rather good agreement with a model they proposed for the quasi 2D biexciton.[27]

Resonant Raman Scattering (RRS), close to the fundamental edge, is difficult to observe in bulk III-V semiconductors, because it is often hidden by strong extrinsic luminescence. To the best of our knowledge excitonic RRS in GaAs has not been reported. In that respect the very weak extrinsic luminescence of GaAs layers in MQWS can be utilized to study excitonic RRS. Moreover, for laser excitation above the $l = 1$ transition ($\hbar\omega_L > E_{11}$) the electrons and holes relax to the bottom of the band producing a luminescence close to E_{11}. It is thus possible to observe RRS on $l>1$ excitons without a luminescence background.

Recently we have studied RRS in GaAs/$Al_{0.3}Ga_{0.7}As$ MQWS with $L_z \sim 100$Å and for a tunable laser excitation covering the E_o, $E_o + \Delta$ range[28]. The Raman cross section exhibits a very sharp resonance at laser photon energy close to the $e-hh$ excition energy, $\hbar\omega_L \sim E_{11}$. The width and position of this resonance is in good agreement with photo luminescence and excitation spectra obtained on the same sample. The $e-lh$ exciton resonance and the outgoing channel ($\hbar\omega_L \sim E_{11} + \hbar\Omega_{ph}$) are hidden by the intrinsic luminescence. However, strong double resonances are observed at the $l = 2$ and 3 transition. The broad widths are most likely due to the inhomogeneous broadening[21] ($\sim l^2$), so that some of the $e-hh$ and $e-lh$ resonances merge together. The resonances on both channels were also observed at the $E_o + \Delta$ gap ($\hbar\omega_L \sim E_o + \Delta$ and $\sim E_o + \Delta + \hbar\Omega_{ph}$). The full spectrum of the Raman cross section is shown in Figure 5. A number of features require more investigation to be completely explained.

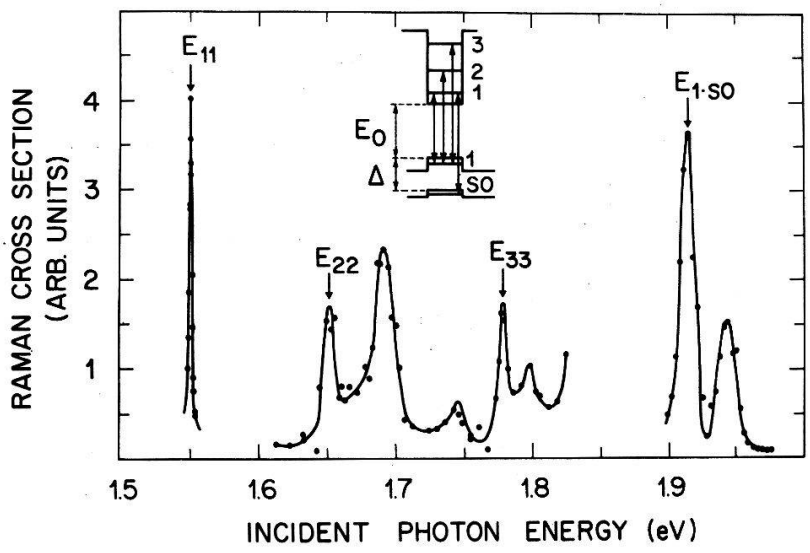

Figure 5: Resonances of the Raman cross section on the $l = 1$, 2, and 3 excitons and at the $E_o+\Delta$ gap in a multiple quantum well structure ($L_z = 102$Å, $L_b = 207$Å, $x = 0.28$).

4. Low Temperature and High Excitation Properties of Quasi-Two-Dimensional Excitons

J. Hegarty et al[29,31] have investigated a number of optical properties of excitons at low temperature, including Resonant Raleigh scattering,[29] spatial hole burning and group velocity reduction[30], and exciton diffusion.[31]

Elastic light scattering in dense media arises from fluctuations of the dielectric constant. The imperfections of the layer thicknesses in MQWS cause local variations of the exciton resonance energy[22,23] and in turn are responsible for fluctuations of the dielectric constant which are particularly important in the strong dispersion domain. Close to the $e-hh$ exciton resonance a dramatic enhancement of the Rayleigh scattering efficiency is observed. Hegarty et al have measured in a $L_z = 51$Å sample an enhancement factor as large as 200 over the off resonance scattering.[29] This impressive result is shown in Figure 6. Assuming a Lorentzian distribution of the exciton resonances they deduced a strong frequency dependence of the homogeneous line width Γ_h within the

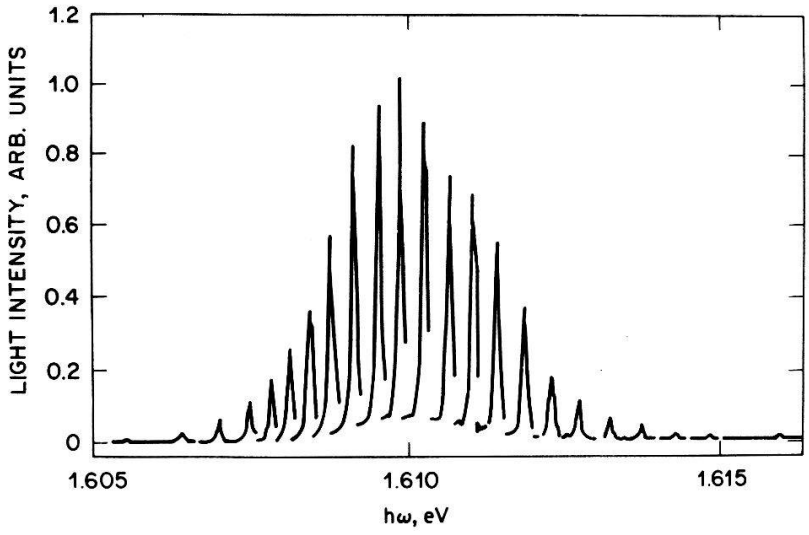

Figure 6: Rayleigh scattering efficiency as a function of the excitation laser frequency for a multiple quantum well structure (L_z = 51Å, L_b = 200Å, x = 0.28) at T = 5.7K. (after Ref. [27]).

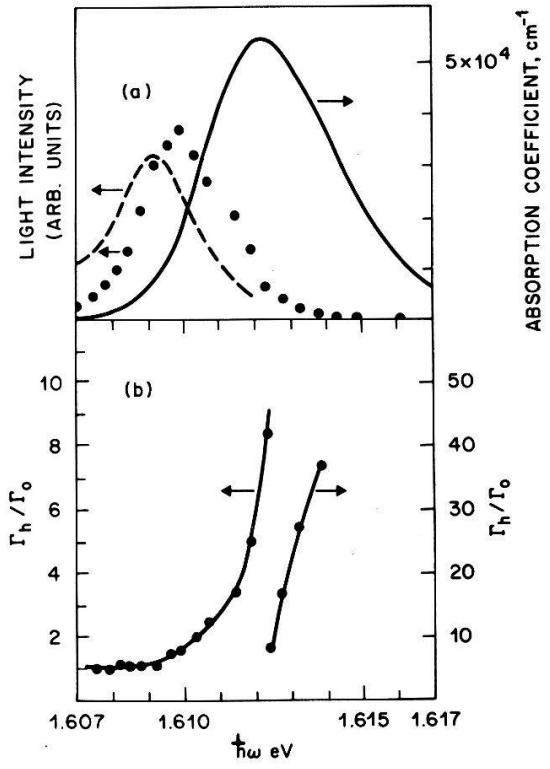

Figure 7: a) Full line: absorption spectrum of the same sample as in Figure 6. Dashed line: nonresonant fluorescence. Points: peak scattered intensity at T = 5.7K.

b) Dependence as a function of energy of the homogeneous line width normalized to the off resonance value. (After Ref. [27]).

inhomogeneous line. Γ_h varies from very small values below the resonance ($\Gamma_h \sim 5\times10^{-2}$ *meV*) to large values above ($\Gamma_h \sim 2$ *meV*). This behavior is shown in Figure 7. They interpreted this result as an indication of exciton delocalization, the low energy excitons being well localized have a narrow homogeneous line width, whereas the high energy excitons are mobile and have a large homogeneous line width.

Using time of flight techniques J. Hegarty has measured on the same sample, *group velocity reduction.*[30] Again the behavior within the inhomogeneous line is unusual; large reduction factors (up to $\sim 2\times10^3$) are observed below the peak of the inhomogeneous line and small ones above. Because of MQWS confinement, polariton effects are restricted to directions of propagation parallel to the plane of the layers (they have not been reported so far). In the direction perpendicular to the layer they are forbidden, and hence the group velocity reduction must have another origin. J. Hegarty found that even at very low intensity hole burning occurs. A narrow hole burned in an inhomogeneous line is equivalent to a negative absorption $\Delta\alpha_k$. Associated with this narrow absorption is a narrow variation of the refractive index and a group velocity $v_g \sim -\Gamma_h/\Delta\alpha_h$, which has the same sign as the measured one. The group velocity reduction is large for small Γ_h. The fact that the measured group velocity varies across the inhomogeneous line width and is smaller below the peak supports the exciton localization interpretation. The dependence of Γ_h with frequency deduced from these experiments agrees well with that obtained from the Resonant Rayleigh measurements.

Low temperature measurements of the dynamics of exciton screening under high excitation conditions were reported by C. V. Shank et al.[32,33] Exciting a MQWS well above the gap with high intensity subpicosecond pulses, they generated electron-hole plasmas. Complete bleaching of the exciton peaks and reduction of the continuum absorption are observed above carrier densities $\sim 0.5\times10^{12} cm^{-2}$. These results are interpreted as due to electron-hole screening of the Coulomb interaction and to band filling effects. The cooling of the hot carrier plasma toward the fundamental edge, corresponding to an electron temperature drop from 600K to the lattice temperature 77K, occurs in approximately 100 ps.

5. Room Temperature Excitons in MQWS

To resolve an exciton from the continuum, the binding energy must be larger than the line width; $B_{1S} > \Gamma$. The line width of an exciton consist of two contributions. One is temperature independent and is the sum of the homogeneous line width and the inhomogeneous line widths induced by crystal imperfections. The temperature dependent contribution arises, in high purity crystals, from the interaction of excitons with thermal phonons. In polar semiconductors it is dominated by the interaction with *LO* phonons. Usually the binding energy and the Frohlich interaction, scale approximately in the same way as a function of the band gap and the ionicity. Thus the condition $B_{1S} > \Gamma$ is only satisfied at low temperature and it is a common belief that in semiconductors Wannier excitons cannot be observed at room temperature.

The electron-phonon interaction in MQWS is slightly modified by the layered structure. Using the infinitely deep well approximation we have calculated the phonon absorption and emission

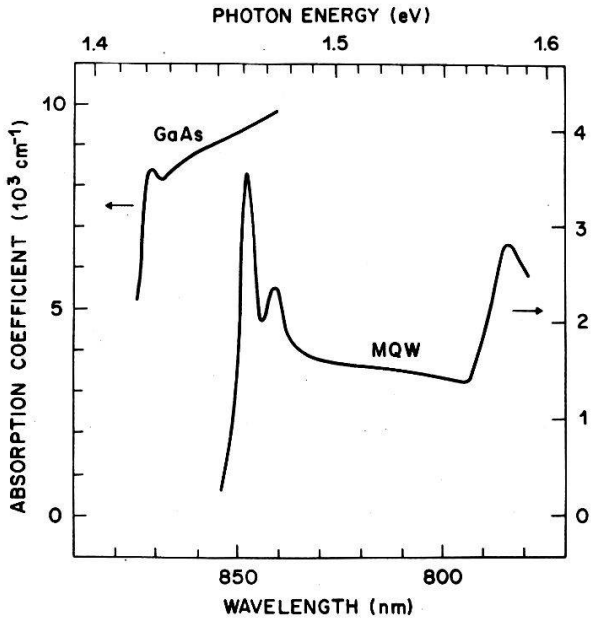

Figure 8: Room temperature absorption coefficient spectra of a 3.2 μm thick high purity GaAs sample and of a multiple quantum well structure. L_z = 102Å, L_b = 207Å, x = 0.28.

rates in MQWS. We found that although an increase of the interaction occurs for very thin layers ($L_z < 50$Å), for layer thickness $L_z \geqslant 100$Å the electron-phonon interaction is approximatively unchanged compared to the bulk. The inhomogeneous broadening of excitons also increases for very thin layers, whereas the confinement enhancement is substantial for $L_z \leqslant a_o$. Therefore a good compromise which allows one to resolve excitons at room temperature is to choose a GaAs layer thickness of the order of a third of the bulk exciton diameter ($L_z \sim 100$Å).

In Figure 8 the room temperature spectrum of a MQWS sample consisting of 77 periods of $L_z = 102$Å GaAs layers and $L_b = 207$ $Al_{.28}Ga_{.72}$ As layers is shown, as is the spectrum of a 3.2 μm thick high purity GaAs sample for comparison.[34] The MQWS spectrum shows the clear double excitonic resonance structure, whereas in the GaAs spectrum the remains of the 3D exciton produces just a slight bump at the band edge. The $e-hh$ exciton binding energy in this sample is approximatively[14] $B_{1S} \sim 9\ meV$. The temperature dependence of the line width of the $e-hh$ exciton, measured as the half width at half maximum on the low energy side of the peak, is shown in Figure 9. It is approximately a constant for temperatures under 150K and increases with tem-

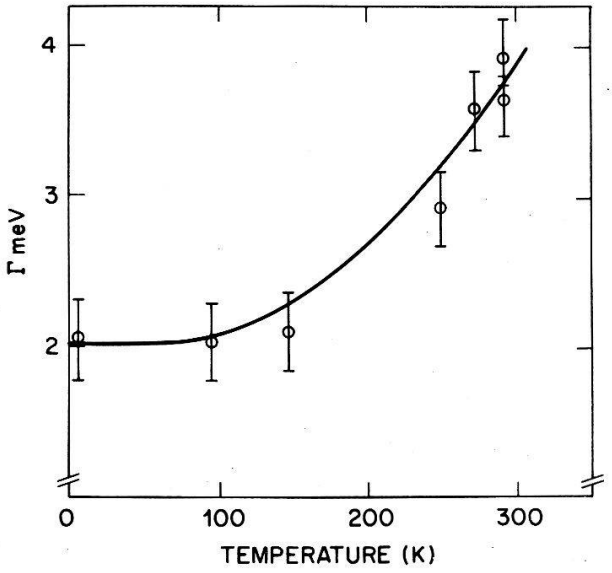

Figure 9: Temperature dependence of the line width of the $e-hh$ exciton in the same sample as in Figure 8.

perature thereafter. The solid line is a fit involving two parameters Γ_o and Γ_{ph} corresponding to the low temperature width and a term proportional to the temperature dependent *LO* phonon density

$$\Gamma = \Gamma_o + \Gamma_{ph}/[exp(\hbar\Omega_{LO}/kT)-1] \tag{11}$$

where $\hbar\Omega_{LO}$ is the GaAs *LO*-phonon energy ($\hbar\Omega_{LO}/k \sim 428K$). The best fit $\Gamma_{ph} = 5.5\ meV$ and $\Gamma_o = 2.\ meV$, is in good agreement with the low temperature luminescence measurements.[21,22] Γ_{ph} is somewhat smaller than that of bulk GaAs[35] ($\Gamma_{ph} \sim 7\ meV$) or that of CdTe[36] ($\Gamma_{ph} \sim 18\ meV$), a semiconductor with band gap and exciton binding energy similar to those of the MQWS sample. It confirms that for these layer thicknesses no enhancement of the exciton *LO* phonon interaction is observed.[22,30]

A number of nonlinear optical effects using excitonic resonant enhancement have been observed in bulk semiconductors. Previously these observations and their applications to optical devices have been limited by the low temperature required to observe excitons. In that respect the possibility of resolving exciton resonances at room temperature in MQWS make these structures particularly interesting. We have studied in detail the nonlinear optical behavior of MQWS at room temperature, near the exciton resonance.[34,38,39] Using cw and pulsed laser excitations we have measured the saturation behavior of the absorption coefficient. An example of cw saturation of the exciton peak for a MQWS and a GaAs reference sample is shown in Figure 10. We have analyzed this data using the usual simple analytical form to characterize the saturation; $\alpha(I) = \alpha_o/[1+I/I_s]$. In the case of GaAs the solid line in Figure 10 corresponds to $\alpha l = 0.5+1.5/(1+I/4.4\times10^3 W/cm^2)$. The behavior of the MQWS sample is more complex, it seems to involve two saturable species since it is well fitted by $\alpha l = 0.35/(1+I/580 W/cm^2) + 0.43/(1+I/4.4\times10^4 W/cm^2)$. Using pulsed laser excitation and gated detection, to eliminate any spurious thermal effects, we have improved these measurements. A summary of our results is given in Table 2. The very low value of the saturation intensity at the exciton peak is confirmed: $I_s \sim 580\ W/cm^2$. Operating our laser in the picosecond regime we have determined the recovery time of the absorption, $\tau_r \simeq 21\times10^{-9}s$.

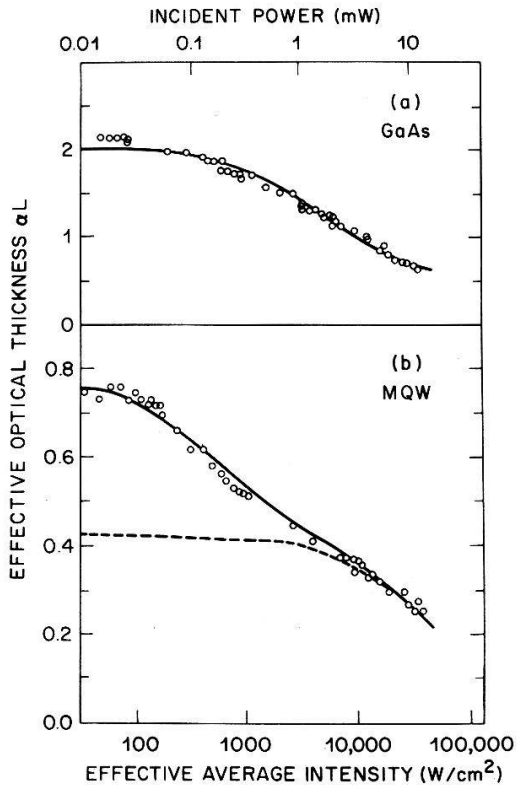

Figure 10: Intensity dependence of optical absorption in a GaAs sample and in a multiple quantum well structure (same parameters as in Figure 8). The solid line correspond to analytical fits discussed in the text.

Energy (eV)	Absorption Coefficient (cm^{-1})	Saturation Intensity (W/cm^2)
1,4595	2420	3680
1,4626	3610	580
1,4642	3380	790
1,4913	1630	$\gtrsim$8000

Table 2: Saturation intensities measured at room temperature around the electron-heavy hole exciton in a multiple quantum well structure. (Well thickness L_z = 102Å, barrier thickness L_b = 207Å. Aluminum content in the barrier layers x – 0,28).

At room temperature excitons exist under rather unusual conditions since

$$kT > B_{1S} > \Gamma \tag{12}$$

Understanding this situation allows us to explain the observed saturation behavior and deserves some comments. Exciton saturation is believed to originate from the screening of the Coulomb interaction. At low temperature, where excitons remain neutral particles, Ulbrich and his coworkers[39] have shown that in thin GaAs samples, very large concentrations (close to 40 times the Mott density) are necessary to shield the Coulomb interaction. At room temperature the phonon contribution to the exciton line width ($\sim 1.8\ meV$) corresponds to a mean time to phonon absorption and therefore to thermal ionization of $t_I = 0.4\ ps$. For steady state excitation, the exciton population is in a thermodynamical equilibrium with electron and hole populations.

$$X \underset{\leftarrow}{\overset{\rightarrow}{}} e + h$$

This situation is similar to that existing in a high temperature hydrogen plasma. It is interesting to note that if the exciton-hydrogen atom analogy is carried one step farther, room temperature for the MQWS exciton ($kT \sim 2.5 \times B_{1S}$) corresponds to $\sim .5 \times 10^6 K$ for hydrogen. The low temperature properties of excitons are those of an exciton gas, (up to a concentration close to the Mott density), whereas at room temperature they are more similar to those of an ionized exciton plasma. To evaluate the concentration of carriers in the steady state we have used the 2D analog of the Saha equation of plasma physics

$$\frac{N_e N_h}{N_X} = \frac{m_e^*}{\pi \hbar^2} kT \exp(-\frac{B_{1S}}{kT}) \tag{13a}$$

where N_e, N_h, N_X are the electron, hole and exciton concentrations. The two other relations to be satisfied are the electrical neutrality condition

(13b) $$N_e = N_h$$

and the particle conservation condition

(13c) $$N_o = N_X + N_h$$

where $N_o = \alpha\tau_r L_z I/\hbar\omega$ is the number of photons absorbed in one layer in the steady state. The solution of Eqs. (13) is shown in Figure 11. The upper curve gives the ionization ratio N_e/N_o and the lower curve gives the concentration of carriers per exciton area $(N_e + N_h)\, A_X$. At low concentration the electrons and the holes generated by thermal ionization have a very small probability of

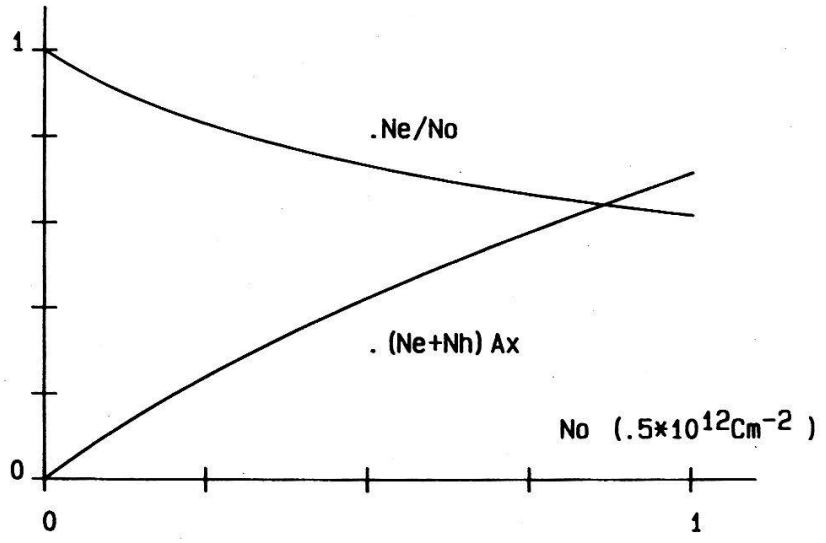

Figure 11: Ionization ratio and number of carriers per exciton area, at thermodynamic equilibrium and steady state excitation, as a function of the number of photons absorbed per layer.

forming an exciton again and $N_e/N_o \rightarrow 1$. At larger densities the number of excitons at equilibrium increases, but N_e/N_o remains larger than 0.6 even at an absorbed photon concentration $N_o \sim 0.5\times10^{12} cm^{-2}$ (i.e., $5\times10^{17} cm^{-3}$) which corresponds approximately to the saturation intensity in the experiments discussed above. At these concentrations the probability of finding one carrier in an exciton area is about 70%.

The screening of the potential of a point charge in a 2D system has been discussed by a number of authors.[40,44] The case of MQWS is somehow intermediate between 2D and 3D because the interaction between layers, which must be accounted for, is not negligible. In a layered system[43,44] the screened potential falls off rapidly at distances above the Bohr radius. In order to obtain results in a closed form, we describe the free carrier screening of excitons by the following crude model. We consider that a point charge sufficiently perturbs the semiconductor locally that no exciton can be generated in an area $A_X = \pi a_o^2$ around it. In the low concentration limit the point defects act independently and Poisson statistics apply. They induce a relative decrease of absorption which is simply $\exp[-(N_e+N_h)A_X]$. The exciton wave function is built up from a surface of the 2D-Brillouin zone which corresponds to wave vectors $|k| \lesssim a_o^{-1}$. Thus the total relative decrease of absorption when N_X excitons are in equilibrium with (N_e+N_h) electrons and holes is;

$$\frac{\alpha(I)}{\alpha_o} \simeq (1 - N_X A_X) \exp[-(N_e + N_h)A_X] \tag{14}$$

where N_X, N_e, N_h are related by Eqs. (13) and are implicit functions of $\alpha(I)$. In the limit $N_o \rightarrow 0$, Eq. (14) reduces to a simple saturation form

$$\alpha(I) = \frac{\alpha_o}{1+\left(\frac{2\tau_r \alpha_o L_z}{\hbar\omega} A_X\right) I} \tag{15}$$

Using the parameters of our sample it leads to;

$$I_s(cal) = 490\ W/cm^2\ . \tag{16}$$

This value is in good agreement with the experimental result.

We can conclude from this discussion that the low saturation intensity of quasi 2D excitons at room temperature originate from the efficient screening of the Coulomb interaction by the electron-hole gas generated through thermal ionization of the excitons.

Associated with any readily saturated absorption is a refractive index which is very sensitive to intensity. In order to determine experimentally this nonlinear refractive index, we have studied the spectral dependence of the nonlinear absorption and Forward Degenerate Four Wave Mixing (FDFWM) efficiency. We use a pump-probe technique with a tunable mode locked laser.[37] An example of the linear transmission, nonlinear absorption and FDFWM efficiency, simultaneously measured on an L_z = 96Å sample is shown in Figure 12. Clear resonances are observed close to the $e-hh$ and $e-lh$ exciton frequencies. At several frequencies, the nonlinear absorption crosses zero whereas the FDFWM efficiency is still large. This observation has been carefully confirmed

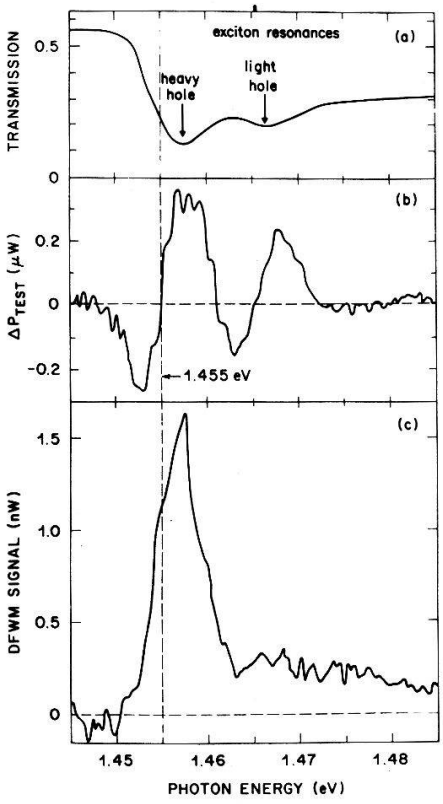

Figure 12: Linear transmission, nonlinear transmission and degenerate four wave mixing spectra for a multiple quantum well structure (L_z = 96Å, L_b = 98Å, x = 0.28).

and is also observed on another sample with L_z = 144Å. The FDFWM can arise either from absorptive or refractive nonlinear effects. At the frequencies where the nonlinear absorption vanishes only the nonlinear refractive index contributes. From our measurements[37] we deduce the variation of the refractive index produced by one electron-hole pair per unit volume; $|n_{eh}| \simeq 2.3\times10^{-19} cm^3$.

The diffraction efficiency we have measured is $\sim10^{-4}$ for sample thickness in the 1−2 μm range and average pump intensity of $\sim30\ W/cm^2$. To the best of our knowledge this is the largest nonlinear optical diffraction efficiency ever reported for a semiconductor at room temperature.

In order to interpret the unusual nonlinear absorption spectrum we have fitted the room temperature linear absorption spectra to empirical line shapes and examined the effects of small variations in the fitting parameters. It was found that the use of Lorentzian line shapes to describe the temperature broadening of the theoretical spectra of Figure 2, gave a poor agreement with experimental data. By contrast excellent fits were obtained using Gaussian line shapes for the excitons and a broadened 2D-Sommerfeld profile for the continuum;

$$\alpha(\omega) = \alpha_h \exp\left[-\frac{(\Omega_h-\omega)^2}{2\Gamma_h^2}\right] + \alpha_l \exp\left[-\frac{(\Omega_l-\omega)^2}{2\Gamma_l^2}\right] + \frac{\alpha_c}{1+exp\left(\frac{\Omega_c-\omega}{\Gamma_c}\right)} \quad \frac{2}{1+exp\left[-2\pi\left(\frac{\Omega_c-\omega}{R_y}\right)^{-1/2}\right]} \tag{17}$$

An example of the quality of the fit is given in **Figure 13.** Attempts to reproduce the shape of the nonlinear absorption spectra by simple variation of the parameters of Eq. (17) failed. Experimentally, when the frequency of the laser is scanned the linear absorption, and therefore the number of carriers generated, varies. Accordingly at each frequency the variations of the parameters induced by the laser should be weighted by the absorption at the same frequency

($\Delta X(\omega) = \Delta X(MAX) \cdot \alpha(\omega)/\alpha(MAX)$). When this procedure is adopted excellent fits are easily obtained, an example of which is shown in **Figure 14**. Very small variations of the parameters are

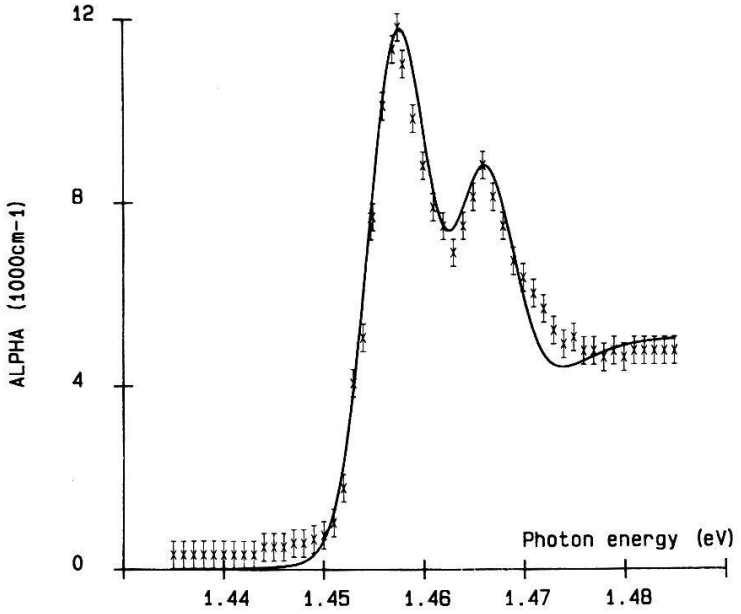

Figure 13: Absorption coefficient spectrum of the same sample. Crosses: experimental data; solid lines fit using the formula discussed in the text.

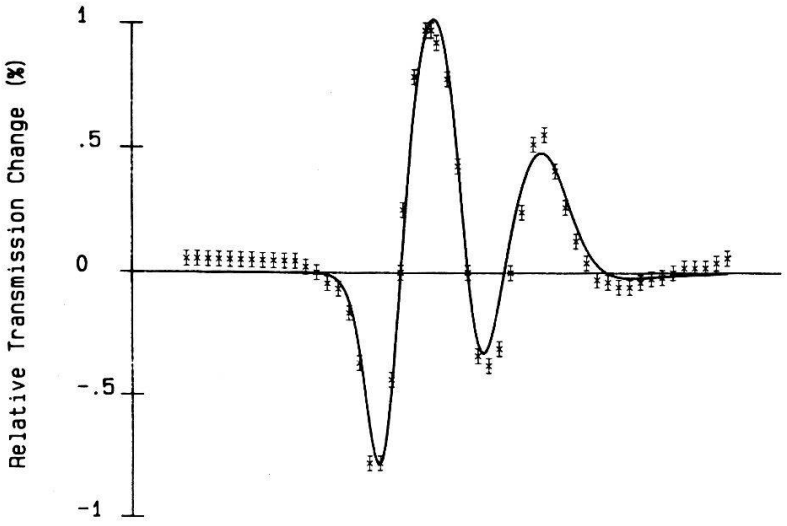

Figure 14: Comparison of the experimental nonlinear transmission spectra (crosses) with a fit obtained by changing the exciton parameters (solid line).

sufficient to reproduce the experimental data, in spite of the extreme sensitivity of the shape of the curve. For $N_o \sim 3\times10^{10}\ cm^{-2}$ photons absorbed per layer ($I \sim 30\ W/cm^2$) it is found that the central frequency of the two excitons shifts by $-5\times10^{-5}\ eV$ and that the relative variations of the peak absorption are -6.3×10^{-2} and -4.8×10^{-2} for the $e-hh$ and $e-lh$ excitons respectively. The $e-hh$ exciton line width broadens slightly by $2\times10^{-4}\ eV$. Variations of the other parameters need not to be considered, in particular the continuum contribution is negligible. These results confirm that the nonlinear optical effects are induced by the free carriers and are simply related to their number. The nature and size of the variations need further investigation.

Room temperature excitons in MQWS are very sensitive to other electro-magnetic perturbations. For instance we have observed electro-absorption due to the Stark effect by application of a static electric field, ξ_o, in the plane of the layers.[38] When a static field is super imposed to the Coulomb potential acting between the electron and the hole, one side of the Coulomb well is lowered and the other raised. This causes shifts, broadening and eventually field ionization for $\xi_o \sim B_{1S}/ea_o$. These effects have been observed in bulk semiconductors at low temperature,[45] but to the best of our knowledge have not been previously observed at room temperature. **Figure 15**

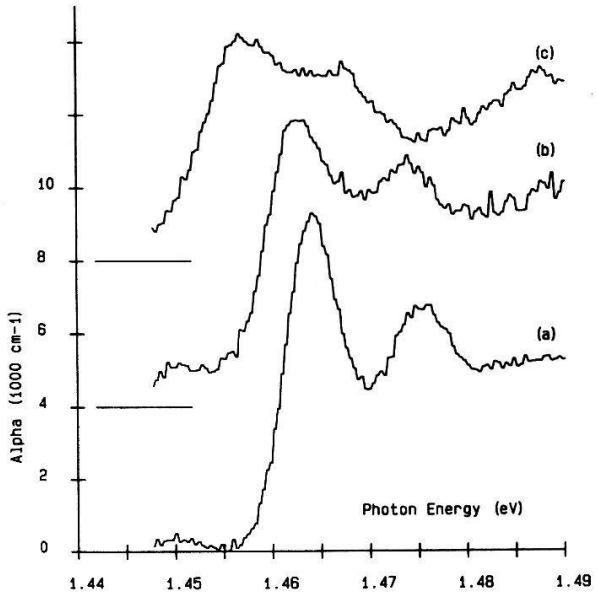

Figure 15: Variation of the absorption spectrum induced by application of a static field parallel to the plane of the layer a) $\xi_o = 0$, b) $\xi_o = 10^4 V/cm$ c) $\xi_o = 1.6\times10^4 V/cm$.

shows the absorption spectra of a sample under a static field $\xi_o = 0 V/cm$, $10^4 V/cm$ and $1.6\times10^4 V/cm$ respectively. Large shifts and broadening are observed for both excitons. They can be utilized to shift a strong absorption into a region that was previously substantially transparent. The magnitude of the effect is one of two orders of magnitude larger than electro absorption, due to Franz-Keldysh effect, in other III-V compounds.

Application of static fields in a direction perpendicular to the layer also modify the optical properties of MQWs. For instance a complete quenching of the excitonic luminescence was observed by Mendez et al[46] when they applied fields of the order of 10 kV/cm in the direction perpendicular to the layers of MQWs. They interpreted their results as a field-induced separation of the electrons and holes.[46]

The observation of large optical nonlinearities at room temperature, for low powers ($< 1\ mW$) and at wavelengths ($\sim 850\ nm$) ideally suited for laser diodes makes the MQWS very attractive candidates for devices systems for optical signal processing,[47] optical communication systems,[48] and high speed image processing.[49] In fact room temperature optical bistability has been recently observed on MQWS,[50] although the intensities at which the device operated were much larger than the exciton saturation intensity. The extreme sensitivity of MQWS absorption to static field can be exploited in high speed amplitude and phase modulation.

Conclusion:

We have reviewed the principal experimental and theoretical results recently obtained on quasi-2D exciton in MQWS. The confinement in the low gap material produces strong modification of the exciton character. In particular excitonic effects are observable at room temperature, leading both to new physical conditions to study these effects and potential applications to utilize them. A number of aspects of quasi-2D exciton physics have not yet understood and need further investigation.

Acknowledgment:

All the work on room temperature excitons in MQWS have been performed in close collaboration with D. A. B. Miller, P. W. Smith, and T. C. Damen. The Resonant Raman studies were made in collaboration with J. Zucker and A. Pinczuk. In both cases we have used samples of very high quality, expertly grown by A. C. Gossard and W. Wiegmann.

I would like also to acknowledge helpful discussions with J. Hegarty, P. F. Liao and R. C. Miller.

REFERENCES

[1] For a recent review see "Electronic properties of two dimensional systems" Proceedings of the 4th international conference on Electronic Properties of Two-Dimensional Systems. Ed. F. Stern, North Holland, Pub. Co. Amsterdam (1982).

[2] L. Esaki, R. Tsu, IBM Res. Dev. *14,* 61 (1970).

[3] A. Y. Cho, J. Vac. Sci. Technol. *8,* 831 (1971).

[4] A. Y. Cho, Appl. Phys. Lett. *19,* 467 (1971).

[5] A. C. Gossard: "Molecular Beam Epitaxy of Superlattices in Thin Films" in "Thin Films: Preparation and Properties" Ed. K. N. Tu and R. Rosenberg, Academic Press, NY (1983).

[6] R. S. Knox, "Theory of Excitons" Sol. State Phys. Sup. 5, Acad. Press, NY (1963).

[7] A. Baladereschi and N. C. LiPari, Phys. Rev. *B3,* 439 (1971).

[8] E. Kane, Phys. Rev. *B11,* 3850 (1975).

[9] R. Dingle, "Confined Carrier Quantum States in Ultra Thin Semiconductor Heterostructures," in Festkörperprobleme XV p. 21, Ed. H. J. Queisser, Pergamon/Vieweg, Braunschweig (1975).

[10] L. Schiff, "Quantum Mechanics", McGraw Hill Book Co., NY (1955).

[11] M. Shinada and S. Sugano, J. Phys. Soc. Jap. *21*, 1936 (1966).

[12] R. Dingle, W. Wiegmann, and C. H. Henry, Phys. Rev. Letters *33*, 827 (1974).

[13] J. M. Luttinger, Phys. Rev. *102*, 1030 (1956).

[14] R. C. Miller, D. A. Kleinman, W. T. Tsang, and A. C. Gossard, Phys. Rev. *B24*, 1134 (1981).

[15] Y. C. Lee and D. L. Lin, Phys. Rev. *B19*, 1982 (1979).

[16] G. Bastard, E. E. Mendez, L. L. Chang, and L. Esaki, Phys. Rev. *B26*, 1974 (1982).

[17] R. Dingle, A. C. Gossard, and W. Wiegmann, Phys. Rev. Lett. *34*, 1327 (1975).

[18] E. Burstein, A. Pinczuk, and S. Buchner, in "Physics of Semiconductors, 1978", Ed. B. L. M. Wilson The Institute of Physics, London (1979).

[19] A. Pinczuk, H. L. Stormer, R. Dingle, J. M. Worlock, W. Wiegmann, and A. C. Gossard, Sol. State Comm. *32*, 1001 (1979).

[20] G. Abstrieter and K. Ploog, Phys. Rev. Lett. *42*, 1308 (1979).

[21] R. C. Miller, D. A. Kleinman, W. A. Norland, and A. C. Gossard, Phys. Rev. *B22*, 863 (1980).

[22] C. Weisbuch, R. C. Miller, R. Dingle, and A. C. Gossard, Sol. State Comm. *37*, 219 (1981).

[23] C. Weisbuch, R. Dingle, A. C. Gossard, and W. Wiegmann, J. Vac. Sci. Technol. *17*, 1128 (1980).

[24] C. Weisbuch, R. Dingle, A. C. Gossard, and W. Wiegmann, Sol. State Comm. *38*, 709 (1981).

[25] R. C. Miller, D. A. Kleinman, O. Munteanu, and W. T. Tsang, Appl. Phys. Lett. *39*, 1 (1981).

[26] W. Brinkman, T. Rice, B. Bell, Phys. Rev. *B8* 1570 (1973).

[27] R. C. Miller, D. A. Kleinman, A. C. Gossard, O. Munteanu, Phys. Rev. *B25* 6545 (1981).

[28] J. Zucker, A. Pinczuk, and D. S. Chemla, to be published.

[29] J. Hegarty, M. D. Sturge, C. Weisbuch, A. C. Gossard, and W. Wiegmann, Phys. Rev. Lett. *49*, 930 (1982).

[30] J. Hegarty, Phys. Rev. *B25*, 4324 (1982).

[31] J. Hegarty, M. D. Sturge, A. C. Gossard, and W. Wiegmann, Appl. Phys. Lett. *40*, 132 (1982).

[32] C. V. Shank, R. L. Fork, B. I. Greene, and C. Weisbuch, Surface Science *113*, 108 (1982).

[33] C. V. Shank, R. L. Fork, R. Yen, J. Shah, B. I. Green, A. C. Gossard, and C. Weisbuch, Sol. State Comm. to be published.

[34] D. A. B. Miller, D. S. Chemla, D. J. Eilenberger, P. W. Smith, A. C. Gossard, and W. T. Tsang, Appl. Phys. Letters *41*, 679 (1982).

[35] V. I. Alperorvch, V. M. Zaletin, A. F. Kravchenko, and A. S. Terekhov, Phys. Stat Solid *B77*, 465 (1976).

[36] V. Segall, Proc. IX Internal Conf. Semicond. Moscow (1968), 425.

[37] D. A. B. Miller, D. S. Chemla, D. J. Eilenberg, P. W. Smith, A. C. Gossard, and W. Wiegmann, to be published in Appl. Phys. Letters.

[38] D. S. Chemla, T. C. Damen, D. A. B. Miller, A. C. Gossard, and W. Wiegmann, to be published in Appl. Phys. Letters.

[39] G. W. Fehrenback, W. Schafer, J. Treusch, and R. G. Ulbrich, Phys. Rev. *49*, 1281 (1982).

[40] F. Stern, Phys. Rev. Lett. *18*, 546 (1967).

[41] F. Stern and W. E. Howard, Phys. Rev. *163*, 816 (1967).

[42] Ando, Fowler, and F. Stern, Rev. Mod. Phys. *54,* (1982).

[43] P. B. Visschu, and L. M. Falicov Phys. Rev. *B3,* 2541 (1971).

[44] A. L. Fetter Ann. Phys. *88,* 1 (1974).

[45] See for example Modulation Spectroscopy by M. Cardona, Solid State Physics Sup. 11. Acad. Press, NY (1969) Chap. VII.

[46] E. E. Mendez, G. Bastard, L. L. Chang, L. Esaki, H. Morkoc, R. Fisher, Phys. Rev. *B26* 7101 (1982).

[47] D. A. B. Miller, Laser Focus *18,* 79 (1982).

[48] P. W. Smith BSTJ *61,* 1975 (1982).

[49] For a recent review see R. A. Fisher (ed), "Optical Phase Configuration" Acad. Press, NY (1983).

[50] H. M. Gibbs, S. S. Tarng, J. L. Jewell, D. A. Weinberger, K. Tai, A. C. Gossard, S. L. McCall, A. Passner, and W. Wiegmann, Appl. Phys. Letters *41,* 221 (1982).